Microstructure measurement based on frequency-shift feedback in a-cut Nd:YVO_4 laser

Weiping Wang (王伟平), Yidong Tan (谈宜东), Shulian Zhang (张书练)*, and Yan Li (李 岩)

Department of Precision Instrument, State Key Lab of Precision Measurement Technology and Instrument, Tsinghua University, Beijing 100084, China

**Corresponding author: zsl@mails.tsinghua.edu.cn*

Received August 11, 2015; accepted October 27, 2015; posted online December 7, 2015

A new optical method based on frequency-shift feedback and laser confocal microscopy is presented to noninvasively measure a microstructure inside a sample. Due to the limit of axial resolution caused by poor signal detection ability, conventional laser feedback cannot precisely measure the microstructure. In this Letter, the light scattered by the sample is frequency shifted before feedback to the laser to obtain a magnification. Weak signals that change with the microstructure can be detected. Together with the tomography ability of laser confocal microscopy, the inner microstructure can be measured with high axial resolution.

OCIS codes: 120.0120, 120.4820, 180.1790, 180.5810.

doi: 10.3788/COL201513.121201.

Microstructures, such as micro-electro-mechanical system devices (MEMS) and binary optical elements, are widely used in fields like biomedicine and the automotive industry. These functional devices always have complex structures, and the packing structure has a layer of protection on the surface. However, the measurement of the microgeometry has an important impact on the performance of the device. Traditional methods, such as the mechanical probe method[1,2], scanning microscopy[3,4], and interferential optical surface profiling[5–7], cannot penetrate into the sample to measure it. The inner structure needs to be corroded from the sample, but then the whole structure will be destroyed. Lee and Li[8] developed submerged optical nanoscopy (SMON) to realize super-resolution imaging of sub-surface nanostructures beyond the optical diffraction limit. In SMON, a highly refractive glass microsphere is immersed in water coupled with a standard optical microscope. However, the radial penetration depth is not sufficient for the measurement. Laser confocal microscopy is a noninvasive optical method to realize tomography measurement, and is usually used to analyze biomedical tissue and cell structures[9,10]. It is also used for microstructure measurement, for example, MEMS technological evaluation[11]. However, due to the restriction on the power of the detected signal, the sample needs to be highly refractive at the lasing wavelength; thus, when using this method, the laser wavelength should be selected in accordance with the sample's reflectivity to this wavelength. Meanwhile, it also cannot achieve a sufficiently high axial resolution for fine microstructure measurements (its axial resolution is more than ten microns).

In 1979, Otsuka was the first to report the remarkable response of a thin-slice $LiNdP_4O_{12}$ laser to Doppler-shifted feedback originating from a rotating ground-glass plate[12]. For a thin-slice solid laser, the power of the feedback light is proven to be magnified by 10^6 when it is frequency shifted by the laser relaxation oscillation frequency[13]. The benefit from this is ultrahigh sensitivity, and the frequency-shift feedback in a microchip laser has significant advantages for weak signal detection and has been widely applied in metrology, such as velocity measurement[12,14], flow measurement[15], particle sizing[16], and displacement sensing[17,18]. In 1999, Lacot *et al.* introduced the frequency-shift feedback of a microchip laser into a scanning confocal system to realize tomography imaging in three-dimensional turbid media[19]. On this basis, Tan *et al.*[20] utilized optical feedback in a microchip Nd:YAG laser and laser confocal microscopy to locate a pin inserted in an onion at a depth of ~3 mm. This method realizes a greater penetration depth than the traditional confocal microscopy with a low light power of less than 1 mW. However, this method still cannot be used in microstructure measurements because the axial resolution is dependent by the FWHM of the defocusing curve, which is 15–20 μm, too low for microstructure measurement. Moreover, in this system, the pump light is projected to an Nd:YAG crystal through optical fiber. Both the deformation and tiny shaking of the optical fiber can cause the change of laser polarization, resulting in the fluctuations of the laser output power to suppress a high axial resolution.

In this Letter, based on the frequency-shift feedback of the Nd:YVO_4 laser and laser confocal microscopy, we propose a novel method to measure a microstructure. The linear relationship between the optical feedback light amplitude and the defocusing amount is first calibrated. When scanning the sample in the lateral direction, the amplitude of the feedback light scattered by the sample changes with the sample structure. By comparing the detected feedback light amplitude with the calibrated linear range, the structure can be measured. In the system, a temperature control setup for the laser is introduced to suppress the laser power fluctuations caused by temperature

 © 2015 Chinese Optics Letters

variations, and an a-cut $Nd:YVO_4$ crystal serves as the light source to ensure the polarization of laser. Thus, power fluctuations caused by laser polarization variation can be avoided. This method has an axial resolution of several nanometers, which is sufficient for microstructure measurement.

The system schematic is shown in Fig. 1(a). A 0.75 mm-thick Nd:YVO4 crystal with 1.1 at.% Nd^{3+} concentration (3 mm × 3 mm) serves as the laser resonator, which is pumped by a laser diode. Both surfaces are coated: the input surface is coated to be highly reflective at the laser wavelength of 1064 nm (R > 99.8%) and anti-reflection coated at the pump wavelength of 808 nm (T > 95%), while the output surface is coated to be 5% transmissive at 1064 nm. In the experiments, this laser works in the single transverse mode and single longitudinal mode. The light (frequency ω) is shifted by two acousto-optic modulators (AOMs) to get the frequency shift Ω, which is the driving frequency difference between the two AOMs. The attenuator (ATT) is an adjustable optical attenuator. The back-scattered light of the sample returns back to the laser via the original path. Thus, the frequency of the light is shifted again to obtain a frequency shift of 2Ω. In the experiments, 2Ω is set to be 2.4 MHz, which is near the laser relaxation oscillation frequency (2.8 MHz), to obtain a proper feedback magnification in the laser. The magnified feedback light is finally detected by a photodiode, and the amplitude information can be demodulated through the lock-in amplifier at a reference frequency of $2\Omega = 2.4$ MHz.

In the experiments, because the diameter of the laser waist is only about 13 μm, the source can be regarded as a point light source. The point source combines with the objective to form a reflection laser confocal system. For an ideal confocal system, the detected intensity can be written as[19]:

$$I(u) = \left|\frac{\sin(u/2)}{u/z}\right|^2, \tag{1}$$

$$u = \frac{8\pi}{\lambda} z \sin^2(\alpha/2), \tag{2}$$

where z is the defocusing of the sample, sin α is the NA of the objective lens, λ is the laser wavelength, and u is the normalized defocusing of the sample.

It has been proven that under weak optical feedback strength, the feedback light-induced laser intensity modulation ΔI can be expressed as[13]

$$\frac{\Delta I}{I_s} = \kappa G(2\Omega)\cos(2\Omega t - \phi + \phi_s), \tag{3}$$

where I_s is the free-running intensity, κ is the effective feedback level, $G(2\Omega)$ is the frequency-dependent amplification, 2Ω is the shifted frequency, φ is the phase of the feedback light, and φ_s is a fixed-phase shift.

For laser confocal feedback system, the combination of Eqs. (1) and (3) can be expressed as

$$\frac{\Delta I}{I_s} = I(u)\kappa G(2\Omega)\cos(2\Omega t - \phi + \phi_s) \tag{4}$$

From Eq. (4), we can get the relationship between the amplitude information A and the defocusing amount $z(A = I(z))$. As shown in Fig. 1(b), with an objective, the defocusing curve $(A = I(z))$ can be obtained when the objective lens is scanned in the longitudinal direction. When scanning, light from the focusing point of the objective lens almost returns back to the laser to obtain the maximum feedback amplitude. Light from defocused positions will be blocked, and the detected light is less. It should be noted that there is an approximately linear region EF in the defocusing curve, which will be used for the measurement. In the measurement, this region is first experimentally calibrated. We focus the light on the sample surface, then move the objective with a certain step in the longitudinal direction, and simultaneously detect the amplitude A. Here, the longitudinal movement of the objective is provided by a one-dimensional motorized scanning stage (provided by Physik Instrumente). The fitted data points to a line and marks the linear region between the amplitude and the defocusing amount. The fitted result is shown in Fig. 1(c). When measuring, we focus the laser beam on a special point of the sample, and then scan the sample in the horizontal direction. During scanning, the amount of feedback light changes with the sample structure variations. By comparing the detected amplitudes with the calibrated linear range, the amplitude information can be converted to the sample structure information.

Because the structure is measured by detecting the light intensity, it is necessary to ensure the laser output's intensity stability in order to obtain a high axial resolution. In the Nd:YAG feedback interferometer, the pump light

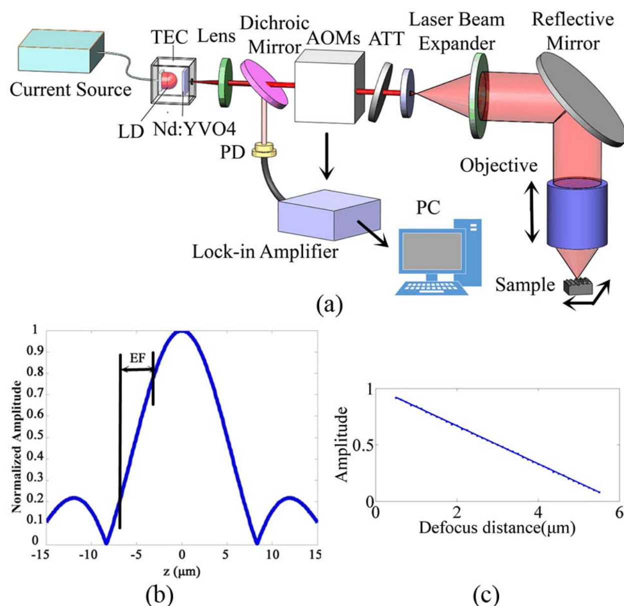

Fig. 1. Configuration and physical principles of the system. (a) The system schematic. (b) The normalized defocusing curve with a certain objective. (c) The calibrated linear range.

source is a fiber-coupled laser diode, and its output is focused on the crystal via a collimating lens. Because the $Nd:YVO_4$ crystal has a wider absorption bandwidth and a higher absorption efficiency than the Nd:YAG crystal, it can be directly pumped. There is no need for the fiber-coupled system. Thus, the laser intensity fluctuation caused by fiber shaking can be eliminated. Moreover, with the integrated design of the pump laser diode and the laser, they can be temperature controlled together by a thermo-electric cooler. The laser intensity drifting caused by temperature fluctuation can be reduced by 60%, as shown in Fig. 2. There is another merit of the $Nd:YVO_4$ crystal. When the $Nd:YVO_4$ crystal is pumped along the a-cut direction, its output is always linearly polarized. The stability of the laser polarization can also improve the stability of the laser output power. Based on above, a high axial resolution can be obtained for microstructure measurements. The axial resolution is measured via the longitudinal movement of the objective at steps on a nanometer scale. As shown in Fig. 3, with different NAs, the different objective lenses result in different linear ranges and different axial resolutions. The experimental measurement axial resolutions are 2, 5, and 11 nm with the objective NA values of 0.65, 0.55, and 0.3. In addition, the lateral resolution is determined by the objective and the wavelength, which can be expressed as $a = 0.61\lambda/(\sqrt{2}\mathrm{NA})$. When NA = 0.65, the lateral resolution is calculated as 0.7 μm, which meets the requirements for microstructure measurement. The axial penetration depth of the system is

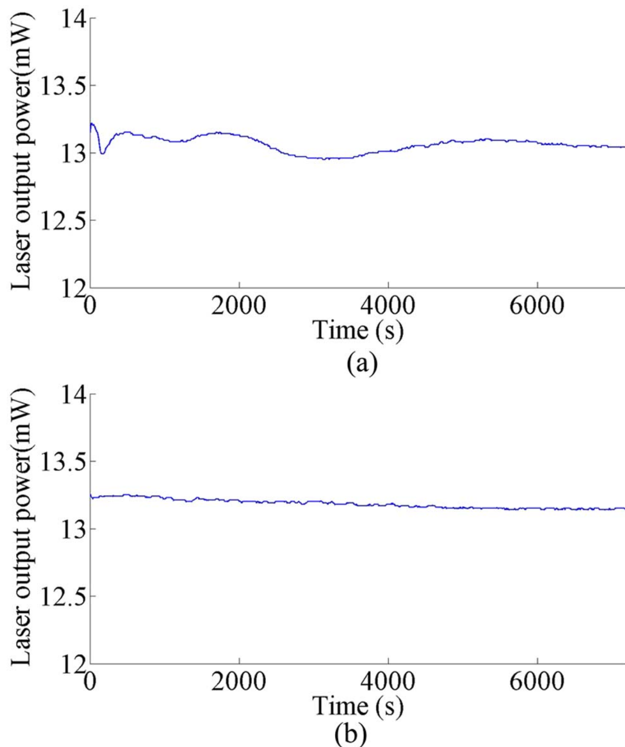

Fig. 2. Nd: YVO_4 laser output power before and after temperature control. (a) Laser output power before temperature control. (b) Laser output power after temperature control.

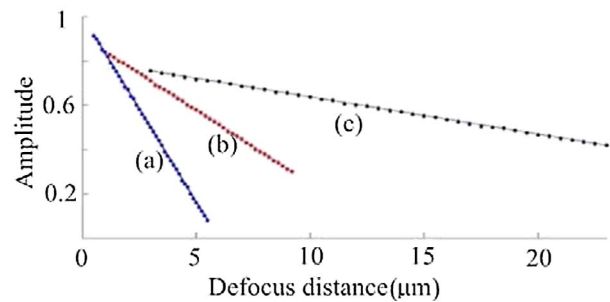

Fig. 3. Normalized linear ranges with different objective lenses. (a) Linear range with the objective of NA = 0.65. (b) Linear range with the objective of NA = 0.55. (c) Linear range with the objective of NA = 0.3.

determined by the working distance of objective lens and the transmittance of the sample surface at the lasing wavelength of 1064 nm. Theoretically, it is only if the light can pass through the surface to the measuring structure that the feedback light scattered by the measuring structure can be detected, because of the ultrahigh sensitivity. Thus, the structure below the surface can be measured. Now, the working range of the objective lens can reach 20.4 mm.

In order to test the reliability of the system, a silicon grating (made by MikroMasch corporation, the period is 3 μm) has been measured. Because the stage height of the grating is about 500 nm, a large NA is chosen to obtain a high resolution. In the experiment, an objective with a magnification factor of 40× and an NA of 0.65 is used. During the measurement, we first focus the light on the grating surface, and then move the objective slightly in the longitudinal direction to ensure that the beginning measurement position is in the linear range. By scanning the sample in the horizontal direction, the amplitude information can be detected. Compared with the calibrated linear range, the amplitude information can be converted into the surface profile. As shown in Fig. 4(b), the stage height of the grating is measured to be 498 nm, while the height measured by the atomic force microscope (AFM) is 493 nm with a 6 nm standard deviation. It should be noted here that because of the limitation of lateral resolution, the high-frequency components of the line profile in Fig. 4(b) are attenuated more than those in Fig. 4(a). The lateral resolution of the system is determined by the NA value of the objective lens and the wavelength; it can be calculated as 1.1 μm by $\mathrm{NA} = 0.61\lambda/(\sqrt{2}\mathrm{NA})$. As shown in Fig. 4(b), the step profile of the grating can be clearly distinguished, and then the transverse resolution can be obtained to about 1 μm by the image analysis of the step. By comparing it with the result measured by the AFM, the reliability of the system has been proven.

A micro-gyroscope is also measured, as shown in Fig. 5(a). The micro-gyroscope is composed of a rotor, metal electrodes, and other microstructures, and a 0.5 mm-thick glass is coated on the surface for protection. Figure 5(b) shows the structure of the rotor in the micro-gyroscope. The rotor has a 270 μm-wide ring structure

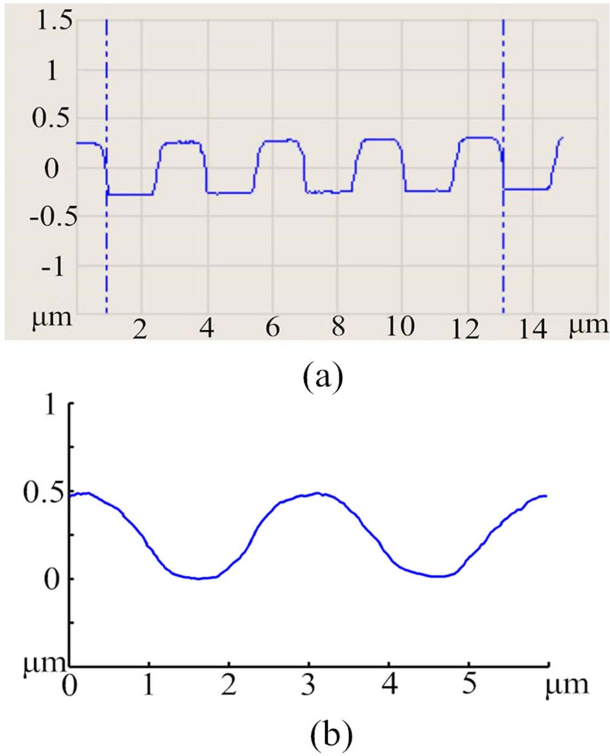

Fig. 4. Measured results of the silicon grating profile. (a) Grating profile measured by AFM. (b) Grating profile measured by our system.

with through-holes in the ring. Our system can realize the noninvasive inner structure measurement through the protection glass, so there is no need to corrode the rotor from the micro-gyroscope. The cross section of the rotor is shown in Fig. 6. According to the actual demands, it is necessary to measure the verticality of the inner side of rotor, which is marked by the circle in Fig. 6. The verticality of the rotor edge is expressed as tilt angel θ between the edge and the sub-face. Actually, the tilt angel θ is designed to be 90°. However, due to an error in the processing, θ cannot be 90° and needs to be precisely measured. Since there is a layer of glass that must be passed through,

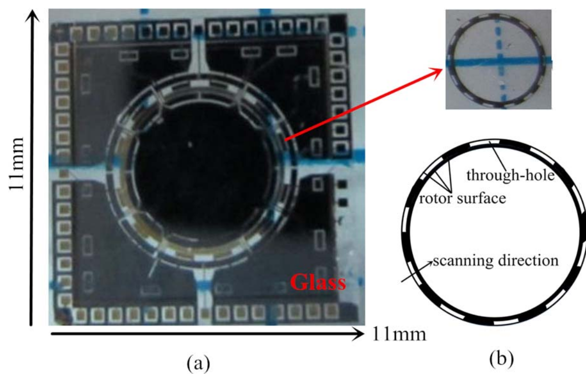

Fig. 5. Physical maps of the micro-gyroscope and the rotor. (a) The micro-gyroscope to be measured. (b) Upper: the rotor corroded from the micro-gyroscope; lower: the top view of the rotor.

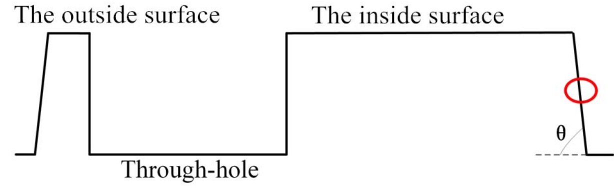

Fig. 6. Cross section of the rotor along the scanning direction in Fig. 5(b). The red circle shows the edge to be measured.

a long-working-distance objective with a magnified factor of 50× and an NA of 0.55, is selected. During measuring, the rotor below the coated glass is firstly located through the longitudinal scanning. Then we slightly move the objective to select a working position, and finally perform a one-dimensional scan of the sample in the horizontal direction.

The measured results are shown in Fig. 7. Two peaks in the measured curve respectively indicate the surfaces of the ring. The valley between the two peaks indicates the through-hole in the ring. In the experiments, according to the vertical and horizontal structure variations of the rotor edge, $\tan(\theta)$ can be calculated, and then θ can be obtained to estimate the verticality of the rotor edge. Three different positions are measured, and the results are listed in Table 1. The data in Table 1 can be used to estimate whether the micro-gyroscope rotor meets the fabrication requirements. During the measurements, the light needs to pass through the coated glass twice, and the light power is mostly lost in the propagation. The feedback light power is much lower than 1 mW. However, due to the magnification of the frequency-shift feedback in the laser, the signal can be still detected to ensure a high vertical resolution.

In conclusion, we present a new method to measure a microstructure, which is based on the tomography ability of laser confocal microscopy and the high sensitivity of the frequency-shift feedback in an a-cut Nd:YVO_4

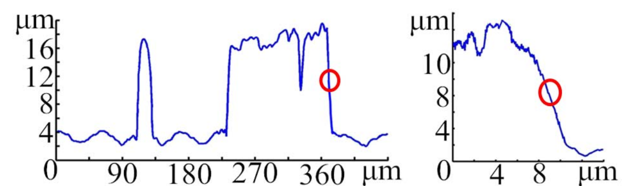

Fig. 7. Measurement results. Left: Lateral scanning diagram of the rotor; right: the edge slope of the rotor.

Table 1. Verticality of Micro-Gyro Rotor

Different Position Numbers	Measured Values
1	84.910°
2	84.671°
3	84.651°

laser. Owing to the high sensitivity of the frequency-shift feedback in the microchip Nd:YVO_4 laser, the linear relation range between the feedback light amplitude and the defocusing distance can be experimentally calibrated. Therefore, the microstructure measurement is converted into a feedback light amplitude measurement. Compared to the traditional laser confocal microscopy, the axial resolution is raised from the tens of microns to the nanometers level. An a-cut Nd:YVO_4 laser is chosen for the laser source to eliminate the light fluctuations caused by polarization change. The source setup is simplified to realize integrated temperature control, which also improves the stability of the system. In this Letter, a silicon grating and a rotor in a micro-gyroscope are measured, which proves the applicability of the system. Other micro-sensors, for example, a micromechanical accelerometer and a micro-flowmeter, can also be measured. Meanwhile, when a microstructure is being used in applied voltage, this method can also be used for the dynamic change measurement of the microstructure.

This work was supported by the National Natural Science Foundation of China (No. 51375262) and the Natural Science Foundation of Beijing (No. 4152024).

References

1. A. Wennerberg, R. Ohlsson, B.-G. Rosén, and B. Andersson, Med. Eng. Phys. **18**, 548 (1996).
2. B.-G. Rosén, L. Blunt, and T. R. Thomas, Proc. J. Phys.: Conf. Ser. **13**, 325 (2005).
3. L. Zhang, T. Sakai, N. Sakuma, T. Ono, and K. Nakayama, Appl. Phys. Lett. **75**, 3527 (1999).
4. V. Kalinin Sergei and A. Gruverman, *Scanning Probe Microscopy: Electrical and Electromechanical Phenomena at the Nanoscale* (Springer Science and Business Media, 2007).
5. J. Schmit and P. Hariharan, Opt. Eng. **46**, 077007 (2007).
6. K. Verma and B. Han, J. Electron. Packag. **122**, 227 (2000).
7. S. Kino Gordon and S. C. Chim Stanley, Appl. Opt. **29**, 3775 (1990).
8. S. Lee and L. Li, Opt. Commun. **334**, 253 (2015).
9. Q. Hu, J. Wang, Z. Fu, X. Mo, X. Ding, L. Xia, Y. Zhang, and Y. Sun, Appl. Microbiol. Biotechnol. **99**, 5605 (2015).
10. J. Hong, W. Guan, G. Jin, H. Zhao, X. Jiang, and J. Dai, Microbiol. Res. **170**, 69 (2015).
11. D. Lellouchi, F. Beaudoin, C. Le Touze, P. Perdou, and R. Desplats, Microelectron. Reliab. **42**, 1815 (2002).
12. K. Otsuka, IEEE J. Quantum Electron. **15**, 655 (1979).
13. R. Kawai, Y. Asakawa, and K. Otsuka, IEEE Photon. Technol. Lett. **11**, 706 (1999).
14. K. Otsuka, Jpn. J. Appl. Phys. **31**, L1546 (1992).
15. S. Sudo, Y. Miyasaka, K. Nemoto, K. Kamikariya, and K. Otsuka, Opt. Express **15**, 8135 (2007).
16. S. Seiichi, M. Yoshihiko, and O. Kenju, Opt. Express **14**, 1044 (2006).
17. W. Xinjun, L. Duo, and Z. Shulian, Opt. Lett. **32**, 367 (2007).
18. Y. Gao, Y. Yu, J. Xi, and Q. Guo, Appl. Opt. **53**, 4256 (2014).
19. E. Lacot, R. Day, and F. Stoeckel, Opt. Lett. **24**, 744 (1999).
20. Y. Tan, W. Wang, C. Xu, and S. Zhang, Sci. Rep. **3**, 2971 (2013).